INSTITUTE FOR FUSION STUDIES

DOE/ER/54346--755

DE-FG03-96ER-54346-755 IFSR #755

Simulation Studies of Acceleration of Heavy Ions and Their Elemental Compositions

MIEKO TOIDA
Department of Physics
Nagoya University
Nagoya 464-01, Japan
and
YUKIHARU OHSAWA[a)]
Institute for Fusion Studies
The University of Texas at Austin
Austin, Texas 78712 USA

[a)] *Permanent address: Dept. of Physics, Nagoya Univ., Nagoya, Japan*

July 1996

THE UNIVERSITY OF TEXAS

AUSTIN

DISCLAIMER

Portions of this document may be illegible in electronic image products. Images are produced from the best available original document.

DISCLAIMER

Simulation Studies of Acceleration of Heavy Ions and Their Elemental Compositions

Mieko Toida

Department of Physics, Nagoya University, Nagoya 464-01, Japan

and

Yukiharu Ohsawa[a)]

Institute for Fusion Studies, The University of Texas at Austin

Austin, Texas 78712 USA

Abstract

By using a one-dimensional, electromagnetic particle simulation code with full ion and electron dynamics, we have studied the acceleration of heavy ions by a nonlinear magnetosonic wave in a multi-ion-species plasma. First, we describe the mechanism of heavy ion acceleration by magnetosonic waves. We then investigate this by particle simulations. The simulation plasma contains four ion species: H, He, O, and Fe. The number density of He is taken to be 10% of that of H, and those of O and Fe are much lower. Simulations confirm that, as in a single-ion-species plasma, some of the hydrogens can be accelerated by the longitudinal electric field formed in the wave. Furthermore, they show that magnetosonic waves can accelerate all the particles of all the heavy species (He, O, and Fe) by a different mechanism, i.e., by the transverse electric field. The maximum speeds of the heavy species are about the same, of the order of the wave propagation speed. These are in good agreement with theoretical prediction. These results indicate that, if high-energy ions are produced in the solar corona through these mechanisms, the elemental compositions of these heavy ions can be similar to that of the background plasma, i.e., the corona.

[a)]Permanent address: Department of Physics, Nagoya University, Nagoya, Japan

I. Introduction

In association with solar flares, high-energy particles are produced (see, for instance, Meyer, 1985ab; Reames, Meyer, and von Rosenvinge, 1994; and references therein). If the particle acceleration is due to a mechanism like Landau damping (Landau, 1946), which is one of the most important processes of energy dissipation in plasmas, the particles with velocities near the wave phase velocity will be accelerated. Thus, the number of accelerated particles may be roughly given by

$$\frac{n_j(h)}{n_j(0)} \sim \exp\left[-\frac{\omega^2}{2(kv_{Tj})^2}\right], \tag{1}$$

where $n_j(0)$ is the background density of ion species j, $n_j(h)$ the density of high-energy particles of species j, ω the wave frequency, k the wave number, and v_{Tj} the thermal speed [for the resonance in a magnetized plasma, see Bernstein (1958)]. Then, in a plasma containing multiple ion species, the fraction of high-energy particles will rapidly decrease with increasing mass, because v_{Tj}^2 is inversely proportional to the mass. That is, the ratio $n_j(h)/n_j(0)$ decreases with mass. In a very high temperature plasma where the ions are fully stripped, the charge-to-mass ratios, q_j/m_j, of heavy ions will be about the same (independent of the ion species j). Even in such a case, the fraction of high-energy particles, $n_j(h)/n_j(0)$, should rapidly decrease with mass (by several orders of magnitude or more).

Observations, however, show that in both gradual and impulsive flares the fraction of high-energy particles does not rapidly decrease with mass. In gradual flares it is almost independent of ion mass (Meyer, 1985ab; Mason, 1987). In impulsive flares it can even slightly increase with mass (Hurford *et al.*, 1975; Mason *et al.*, 1986; Reames, 1990; Reames, Meyer, and von Rosenvinge, 1994).

The acceleration mechanisms may not be as simple as the Landau damping. However, the discrepancy between Eq. (1) and the observations shows that acceleration models must account for the fact that in energetic particles in either impulsive or gradual flares the relative abundance of heavy ions are not depleted and are, roughly speaking, almost independent of their masses.

It is well known that interplanetary (magnetosonic) shocks can accelerate particles (Sarris and Krimigis, 1985). Theory and simulations also show that large-amplitude magnetosonic waves can promptly accelerate ions to high energies (Tokar, Gary, and Quest, 1987; Lembege and Dawson, 1989; Ohsawa, 1990). Thus magnetosonic waves could also produce high-energy particles in strong plasma disturbances in solar flares (Ohsawa and Sakai, 1987). However, these theoretical and simulation studies were made on plasmas with single ion species. If magnetosonic waves play dominant roles in the acceleration processes in solar flares, they must be able to accelerate heavy ions as well as hydrogens. In this paper we discuss the mechanism of accelerating heavy ions by magnetosonic waves.

In a magnetosonic wave the change in the electric potential is quite large; for a perpendicular wave it is $e\varphi \approx 2m_i v_A^2(M-1)$, where m_i is the ion mass, v_A the Alfvén speed, and M the Alfvén Mach number (Adlam and Allen, 1958; Davis *et al.*, 1958). In a single-ion-species plasma, this large potential can reflect some fraction of ions and accelerate them to high energies (Ohsawa, 1990). However, if we apply the same mechanism to heavy ions in a multi-ion-species plasma, we find that the fraction of reflected ions exponentially decrease with mass, like Eq. (1) (Toida, Zhang, and Ohsawa, 1992). This is because thermal speeds of heavier ions are much smaller than the wave propagation speed, which is about the Alfvén speed.

Recently particle simulations for a two-ion-species plasma were performed (Toida and Ohsawa, 1995), in which hydrogen and helium were contained with the number-density ratio $n_{He}/n_H = 0.1$. Those simulations showed that heavy ions (He) as well as light ions (H) can be accelerated by magnetosonic waves and that their mechanisms are completely different. As in a single-ion-species plasma, hydrogens are accelerated through reflection by electric potential. On the other hand, heavy ions are accelerated to the direction parallel to the wave front by transverse electric fields.

In this paper, in order to compare more directly and more clearly with observations, we will carry out simulations, increasing the number of ion species up to four. In Sec. II, we will give a physical argument on the mechanism of heavy ion acceleration by magnetosonic waves. In Sec. III, by using a one-dimensional, fully electromagnetic particle code with full ion and electron dynamics, we study ion acceleration by magnetosonic waves propagating perpendicular to a magnetic field in a plasma containing four ion species: H, He, O, and Fe.

As in the solar plasma, the number-density ratio n_{He}/n_H is 0.1, and the abundance of O and Fe are taken to be much smaller than those of H and He. It will be shown that heavy ions (He, O, and Fe) are accelerated by the mechanism different from that of hydrogen. All the particles of all the heavy species are accelerated. All of them have about the same maximum speed; it is about the wave propagating speed. In Sec. IV, we will see that oblique magnetosonic waves can also accelerate ions in a similar way. Section V will give a summary of our work. These simulations show that the fraction of ions accelerated by magnetosonic waves, $n_j(h)/n_j(0)$, can be almost independent of ion species j, which is in agreement with the observations that elemental compositions of solar energetic particles are similar to that of the corona.

II. Physical Argument

Here we will give physical pictures of ion acceleration by magnetosonic waves. First, we describe some properties of magnetosonic waves in a two-ion-species (H and He) plasma. In space plasmas, other heavy ion species such as Fe are also contained. Their abundance are, however, quite small compared to those of H and He. Thus, their effects on the wave structure will be neglected. Next, we will discuss acceleration of hydrogen and heavy ions by these waves. The mechanism of heavy ion acceleration presented here is applicable to O, Fe, etc., as well as to He.

A. Wave propagation

We consider magnetosonic waves propagating perpendicular to a magnetic field in a plasma consisting of electron, hydrogen, and helium; the number density of He will be assumed to be 10% of that of H. In a two-ion-species plasma, the magnetosonic wave is split into two modes (Buchsbaum, 1960); we here call them low- and high-frequency modes. Their dispersion curves are shown in Fig. 1, where Ω_H is the hydrogen cyclotron frequency, c the speed of light, and ω_{pe} the electron plasma frequency; the low- and high-frequency modes are denoted by ω_- and ω_+, respectively. The frequency ω of the low-frequency mode goes to zero as the wave number k tends to zero and approaches the ion-ion hybrid resonance frequency ω_{-r} as $k \to \infty$. The high-frequency mode has a finite cutoff frequency ω_{+o} at

$k = 0$ and has a resonance frequency ω_{+r} about the lower-hybrid resonance frequency as $k \to \infty$. We have the following relation among these cutoff and resonance frequencies and the cyclotron frequencies of He and H:

$$\Omega_{He} < \omega_{-r} < \omega_{+o} < \Omega_H. \tag{2}$$

The resonance frequency ω_{+r} is about $(m_H/m_e)^{1/2}$ times as large as the hydrogen cyclotron frequency Ω_H, unless the plasma density is very low; here m_H is the hydrogen mass, and m_e the electron mass. The expressions for these frequencies can be found in, for instance, Toida and Ohsawa (1994).

For large-amplitude waves, the high-frequency mode is more important than the low-frequency mode (Toida, Ohsawa, and Jyounouchi, 1995). Thus, in the following we mainly discuss the high-frequency mode and will call it the magnetosonic wave. In the range of wave numbers

$$(m_e/m_H)^{1/2} \ll c^2k^2/\omega_{pe}^2 \ll 1, \tag{3}$$

this mode is given by

$$\omega_+ = v_h k\,[1 - c^2k^2/(2\omega_{pe}^2)]. \tag{4}$$

The quantity v_h gives a measure of the propagation speed of magnetosonic wave in this range of wave numbers and is defined as

$$v_h = \frac{(\omega_{pH}^2 + \omega_{pHe}^2)^{1/2}|\Omega_e|c}{\omega_{pe}^2} = v_A\left[1 + \frac{\omega_{pH}^2\omega_{pHe}^2}{\omega_{pe}^4}\Omega_e^2\left(\frac{1}{\Omega_H} - \frac{1}{\Omega_{He}}\right)^2\right]^{1/2}. \tag{5}$$

Here, ω_{pj} is the plasma frequency for hydrogen (j=H), helium (j=He), or electron ($j = e$), and v_A is the Alfvén speed

$$v_A = B_o/[4\pi(n_H m_H + n_{He} m_{He})], \tag{6}$$

with B_o the strength of the external magnetic field. The speed v_h is slightly greater than the Alfvén speed v_A, and in a single-ion-species plasma it reduces to v_A.

It is well known that in a single-ion-species plasma, nonlinear magnetosonic waves can be described by the Korteweg-de Vries (KdV) equation (Gardner and Morikawa, 1965). Even though in a two-ion-species plasma, the (high-frequency) magnetosonic wave has a finite cutoff frequency, it can also be described by a KdV equation unless the wave amplitudes are too small (Toida and Ohsawa, 1994). The nonlinear theory gives the potential jump φ in a magnetosonic shock wave as

$$e\varphi \sim \frac{m_e}{m_H \eta^2 \alpha} 2 m_H v_h^2 (M-1), \tag{7}$$

where M is the Mach number (Mv_h is the propagation speed), η is a quantity of the order of $(m_e/m_H)^{1/2}$,

$$\eta = (\omega_{pH}^2 + \omega_{pHe}^2)^{1/2}/\omega_{pe}, \tag{8}$$

and α is a constant about unity

$$\alpha = 1 + \frac{\omega_{pH}^2 \omega_{pHe}^2 (\Omega_H - \Omega_{He})^2}{(\omega_{pH}^2 + \omega_{pHe}^2)^2 \Omega_H \Omega_{He}}. \tag{9}$$

The quantity $m_e/(m_H \eta^2 \alpha)$ is also about unity, and it becomes exactly unity when the helium density is zero.

This potential produces a longitudinal electric field in the direction of the wave normal. Because the magnetic field in a magnetosonic wave changes with time, there is also a transverse electric field in the direction parallel to the wave front. Its magnitude is

$$E \sim (2/\alpha)(v_h B_o/c)(M-1). \tag{10}$$

B. Hydrogen acceleration

We now consider a plasma containing H, He, and heavier ions such as Fe. The number density of He is again about 10% of that of H. The abundance of heavier ions are assumed to be much smaller than those of H and He. The electric potential formed in a magnetosonic wave can reflect some fraction of ions and accelerate them to high energies. This mechanism has been studied in detail for a single-ion-species plasma by many authors (Biskamp and Welter, 1972; Forslund *et al.*, 1984; Tokar *et al.*, 1987; Lembege and Dawson, 1989; Ohsawa, 1990).

In multi-ion-species plasmas, some fraction of light ions (H) can be accelerated by the same mechanism. If a particle is reflected once, its speed will reach the value $v \sim 2Mv_h$, (Ohsawa, 1990) (the maximum speed depends on the number of reflections). The fraction of ions reflected by the potential is

$$n_{jref}/n_{jo} \sim \exp[-v_{jref}^2/(2v_{Tj}^2)], \tag{11}$$

where n_{jref} is the density of reflected ions of j-th species, n_{jo} the background density, v_{Tj} the thermal velocity, $v_{Tj} = (T_j/m_j)^{1/2}$, and v_{jref} the minimum velocity for the reflection,

$$v_{jref} = Mv_h - \left(\frac{4m_e}{m_H \eta^2 \alpha} 2v_h^2 (M-1) \frac{Z_j^*}{A_j} \right)^{1/2} . \tag{12}$$

Here, Z_j^+ is the charge of ion j, A_j the mass number. The quantity v_{jref} is of the order of v_h, and its dependence on heavy species is rather weak. Because heavy ions have small thermal velocities, we see from Eq. (11) that the fraction n_{jref}/n_{jo} decreases rapidly with increasing mass m_j.

C. Heavy ion acceleration

Longitudinal electric field can hardly reflect ions with large masses. Nevertheless, heavy ions can be accelerated by magnetosonic waves by a different mechanism (Toida and Ohsawa, 1995). The acceleration is made by the transverse electric field in the wave.

To discuss this mechanism, we consider a magnetosonic shock wave propagating in the x direction in a magnetic field that points in the z direction (see Fig. 2). The perturbed magnetic field ($\widetilde{B}_z = B_z - B_o$), electric potential ($\varphi$), and transverse electric field (E_y) have similar profiles, and in the shock ramp they all sharply rise. In a magnetosonic wave in a single-ion-species plasma, the fluid ion velocity in the x direction, v_{ix}, is equal to the fluid electron velocity, v_{ex}, everywhere and they both satisfy the relation (Adlam and Allen, 1958; Davis *et al.*, 1958)

$$E_y - \frac{v_{jx} B_z}{c} \approx 0, \tag{13}$$

where the subscript j refers to particle species. Even in a multi-ion-species plasma, hydrogen ions, which are the majority ion species, and electrons can approximately satisfy the above relation. When they encounter the shock, their v_{jx} quickly change so that the above relation holds in the shock region as well as in the upstream and downstream regions. However, heavy ions, which are minority components, cannot satisfy Eq. (13), because they cannot respond to the wave so quickly. Consequently, when they encounter the shock wave, their values of v_{jx} stay nearly equal to zero for a long time. We then see from the y component of the equation of motion,

$$\frac{dv_{jy}}{dt} = \frac{q_j}{m_j} \left(E_y - \frac{v_{jx} B_z}{c} \right), \tag{14}$$

that v_{jy} significantly increases because of the transverse electric field E_y ($E_y > 0$).

The velocity v_{jy} is gradually converted to v_{jx} by the Lorentz force, and when v_{jx} is substantially increased, this acceleration will cease. Thus, the acceleration time Δt will be

$$\Delta t \sim 1/\langle \Omega_j \rangle, \tag{15}$$

where $\langle \Omega_j \rangle$ is the average cyclotron frequency of ion j during this time period. Let B_m be the maximum magnetic field strength; then $\langle \Omega_j \rangle$ can be estimated as

$$\langle \Omega_j \rangle \sim \frac{q_j}{m_j c} \frac{(B_m + B_o)}{2}. \tag{16}$$

Neglecting the second term in the right-hand side of Eq. (14), we have the maximum speed v_{jym}

$$v_{jym} \sim \frac{q_j}{m_j} \frac{\delta E_y}{2} \Delta t, \tag{17}$$

where δE_y is the increase in E_y during δt, and thus $\delta E_y/2$ is the average E_y; δt is the time period for which, for instance, the magnetic field rises from B_o to B_m [we can define δx as the corresponding length (i.e., shock width)]. Faraday's law gives the relation between δE_y and the change in the magnetic field, $(B_m - B_o)$:

$$\delta E_y \sim \frac{\delta x}{\delta t} \frac{B_m - B_o}{c}. \tag{18}$$

Because the quantity $\delta x/\delta t$ is estimated by the wave propagation speed, $\delta x/\delta t \sim M v_h$, it follows from Eqs. (15)–(18) that

$$v_{jym} \sim \left(\frac{B_m - B_o}{B_m + B_o} \right) M v_h. \tag{19}$$

The maximum speed can easily exceed v_h or the Alfvén speed. This mechanism should be applicable to all the heavy ions (i.e., all the particles of all the species heavier than H); they all have the same maximum speed given by the above equation.

So far, we have discussed the acceleration mechanism seen in the laboratory frame. Now let us briefly describe the same process in the wave frame where the wave form is stationary ($\partial/\partial t = 0$). In such a frame, the plasma is moving from $x = \infty$ to $x = -\infty$. The electric field in the y direction becomes constant in time and space and is given by $E_{yo} = -M v_h B_o/c$. Thus instead of Eq. (14), we have the equation of motion as

$$\frac{dv_{jy}}{dt} = -\frac{q_j}{m_j} \left(\frac{M v_h B_o + v_{jx} B_z}{c} \right). \tag{20}$$

In the upstream region, guiding centers of all the particle species flow with the same speed; it is

$$v_x = cE_{yo}/B_z(x), \tag{21}$$

and, at $x = \infty$, it is $v_x = -Mv_h$. When the particles enter the pulse region where the magnetic field is strong, electrons and hydrogens are quickly decelerated (because of Eq. (21)); hence the right hand side of Eq. (20) is nearly zero in the pulse region as well as in the upstream region. However, heavy ions cannot be decelerated so quickly. They penetrate the pulse region keeping their velocity ($-Mv_h$) almost unchanged for a while. Substituting $v_{jx} = -Mv_h$ in Eq. (20), we find that v_{jy} can rapidly increase in the pulse region. Using the acceleration time (15), we can derive the maximum speed same as (19).

III. Simulations of Heavy Ion Acceleration

In this section we discuss the heavy ion acceleration by a magnetosonic wave, using particle simulation. This method enables us to study various phenomena and effects (wave propagation, particle acceleration, presence of multi ion species, etc.) in a self-consistent manner.

A. Simulation model

We use a one-dimensional (three velocity components), fully electromagnetic particle code with full ion and electron dynamics. The total grid size is $L_x = 4096\Delta_g$, where Δ_g is the grid spacing. All lengths and velocities in the simulations are normalized to Δ_g and $\omega_{pe}\Delta_g$, respectively, where ω_{pe} is the spatially averaged plasma frequency. The simulation particles are confined in the region $100 < x < 3996$, being specularly reflected at $x = 100$ and $x = 3996$. Outside the plasma region, electromagnetic radiation leaving the plasma region is absorbed; thus we can avoid the interactions between the left and right sides of the plasma regions through the vacuum region (Liewer *et al.*, 1981). Shock waves excited in this system propagate in the positive x direction (for the method of excitation of shock waves, see Toida and Ohsawa, 1995). In the upstream region, all the particle species have isotropic Maxwellian velocity distribution functions.

We simulate a multi-ion-species plasma containing hydrogen (H), helium (He), oxygen(O), and iron (Fe). Assuming the plasma temperature $T \approx 2 \times 10^6$ K, we choose the ratios of ion cyclotron frequencies as $\Omega_{He}/\Omega_H = 1/2$, $\Omega_0/\Omega_H = 7/16$, and $\Omega_{Fe}/\Omega_H = 1/4$. As in the solar plasma, the abundance of heavy ions are set to be quite small. The abundance ratio of helium to hydrogen is $n_{He}m_{He}/(n_H m_H) = 4 \times 10^{-1}$, where n is the number density and m is the mass. The abundance of oxygen and iron are $n_O m_O/(n_H m_H) = 4 \times 10^{-3}$ and $n_{Fe}m_{Fe}/(n_H m_H) = 2 \times 10^{-3}$. To have accurate statistical data of ions with very small abundance, we have used the simulation technique of fine particles, which is described in the Appendix.

The number of simulation particles is $N_e = 144276$ for electrons. The numbers of ion particles are determined according to their abundance; in the total system the plasma is electrically neutral. Other simulation parameters are the following: The hydrogen-to-electron mass ratio is $m_H/m_e = 50$, and the light speed is $c = 4$. The electron thermal velocity is $v_{Te} = 1.0$. Ion thermal velocities are $v_{TH} = 0.14$, $v_{THe} = 0.071$, $v_{TO} = 0.035$, and $v_{TFe} = 0.019$. The strength of the external magnetic field is chosen so that $|\Omega_e|/\omega_{pe} = 1.5$. For these parameters, the beta value, which is defined as the ratio of the plasma pressure to the magnetic energy, is $\beta = 0.05$, and the Alfvén speed is $v_A = 0.78$. The velocity v_h, which is given by Eq. (5) and is a measure of the propagation speed of a magnetosonic wave in a multi-ion-species plasma, is $v_h = 1.03 v_A = 0.80$. The hydrogen gyro-radius is $\rho_H = 4.7$ and the electron skin depth is $c/\omega_{pe} = 4$.

B. Perpendicular waves

Let us now discuss simulation results. We show in Fig. 3 time evolution of magnetic field profiles ($B_z(x)/B_o$) in a nonlinear magnetosonic pulse (quasi-shock wave) propagating perpendicular to a magnetic field in a multi-ion-species plasma. The speed of this pulse is observed to be $v = 2.0 v_h$ ($= 2.1 v_A$). The magnetic field sharply rises in the shock region.

Three upper panels in Fig. 4 show snapshots of the magnetic field B_z, longitudinal electric field E_x, and transverse electric field E_y; the magnetic and electric fields are normalized to B_o and $v_h B_o/c$, respectively. As mentioned earlier, the transverse electric field has a profile similar to that of the magnetic field. Four lower panels are phase-space plots (x, v_y) of ions;

the velocities are normalized to v_h. They show hydrogen, helium, oxygen, and iron. All ion species are strongly accelerated by the magnetosonic pulse. Some of the hydrogens are reflected at the wave front by the longitudinal electric field E_x and gain a lot of energy. Their acceleration is very quick. On the other hand, the heavy ions (He, O, and Fe) are accelerated by the transverse electric field E_y, and their energies increase rather slowly compared to those of hydrogen. Furthermore, among the heavy ions, particles with lower charge-to-mass ratios gain kinetic energy more slowly, with time scale $\sim \langle \Omega_j \rangle^{-1}$. Heavy ion species have about the same maximum speed. It is $v \sim 0.9 v_h$ in the pulse region; if we substitute the values $M = 2.0$, $B_m/B_o = 2.5$ in Eq. (19), we also have $v \sim 0.9 v_h$. Another important point is that the acceleration takes place with all the heavy ions (all the particles in all the heavy species).

Figure 5 shows phase-space plots (v_x, v_y) of H, He, O, and Fe. This also clearly indicates that for heavy ions all the particles are accelerated, while for hydrogen ions, some fraction of particles are accelerated. Here the particles that were present in the region from $x/(c/\omega_{pe}) =$ 780 to 840 at $\omega_{pe} t = 1750$ were plotted. However, for Fe, a longer region is taken, from $x/(c/\omega_{pe}) = 675$ to 840, because the acceleration is slower.

We have examined some important features of heavy ion acceleration: maximum speed, its independence on the species, acceleration of all the heavy particles, etc. These results are in good agreement with the theoretical prediction in the previous section.

C. Oblique waves

So far we have discussed perpendicular waves, for which the theory is rather simple as described in Sec. II. Let us now study oblique waves by means of particle simulations.

Figure 6 shows snapshots of field profiles and phase-space plots for a magnetosonic wave propagating obliquely with the angle $\theta = 50°$ (angle between the external magnetic field and the wave normal); the wave propagation speed is $v = 2.1 v_h$ ($= 2.2 v_A$). Other simulation and physical parameters are the same as those for Fig. 4. It is found from Fig. 6 that strong acceleration of hydrogen and heavy ions can also occur in an oblique wave; some of the hydrogen ions are reflected by the longitudinal electric field E_x, and all the particles of all the heavy species gain energies from the transverse electric field E_y. Again, all the heavy ion species have about the same maximum speed. It is of the order of the propagation speed of the pulse.

IV. Summary

We have studied heavy ion acceleration caused by magnetosonic waves in multi-ion-species plasmas. First, we gave physical pictures of ion acceleration and predicted the maximum speed of heavy ions. Then, a one-dimensional, electromagnetic particle simulation code was used to investigate this mechanism in a self-consistent manner. The simulation plasma has four ion species: H, He, O, and Fe. The abundance of He was taken to be 10% of that of H, and those of O and Fe were much smaller than that of H (or He). It was shown that magnetosonic waves can accelerate heavy ions (He, O, and Fe) as well as hydrogen ions. The acceleration mechanisms of heavy ions and of hydrogen are different. The hydrogen ions are accelerated by the longitudinal electric field in the magnetosonic wave, and only a small fraction of particles are accelerated. On the other hand, heavy ions gain energies from the transverse electric field. All the particles of all the heavy species are accelerated. Furthermore, their maximum speeds, which are of the order of the wave propagation speed, are about the same, almost independent of particle species. These are in good agreement with theoretical predictions. In addition, simulations confirmed that the heavy ion acceleration can take place in either perpendicular or oblique waves. Our results suggest that, if this acceleration occurs somewhere in the solar corona, the high-energy heavy ions will be observed to have an elemental composition similar to that of the background plasma, i.e., the corona.

Appendix

In a space plasma, the abundances of heavy ions such as oxygen and iron are quite small compared to those of electron and hydrogen. In particle simulations we can use only a limited number of particles; in the present simulations, the number of electrons is $N_e \sim 1.4 \times 10^5$. Thus the number of heavy ions used in the simulation must be very small. However, to accurately model those particles from a statistical point of view, a large number of particles is desirable. To increase the number of simulation particles for each heavy ion species, we use fine particles: i.e., we make the mass and charge of a simulation particle small, keeping the charge-to-mass ratio q_j/m_j and the abundance $n_j m_j$ unchanged (Ohsawa and Dawson, 1984). Specifically, we have used the mass and charge ratios as follows: $m_O/m_H = 1/25$, $m_{Fe}/m_H = 11/500$, $q_O/q_H = 7/400$, and $q_{Fe}/q_H = 11/2000$. The numbers of simulation particles are $N_O = 12000$ and $N_{Fe} = 12000$.

Acknowledgments

One of the authors (Y.O.) is grateful to Dr. James Van Dam for warm hospitality and stimulating discussions during his visit to the Institute for Fusion Studies, The University of Texas at Austin. This work was supported in part by the U.S.-Japan Joint Institute for Fusion Theory.

References

Adlam, J.H., and Allen, J.E. 1958, Philos. Mag. **3**, 448.

Bernstein, I.B. 1958, Phys. Rev. **109**, 10.

Biskamp, D., and Welter, H. 1972, Nuclear Fusion **12**, 663.

Buchsbaum, S.J. 1960, Phys. Fluids **3**, 418.

Davis, L., Lüst, R., and Schulüter, A. 1958, Z. Naturforsch. Teil A **13**, 916.

Forslund, D.W., Quest, K.B., Brackbill, J.U., and Lee, K. 1984, J. Geophys. Res. **89**, 2142.

Gardner, C.S., and Morikawa, G.K. 1965, Commun. Pure Appl. Math. **18**, 35.

Hurford, G.J., Mewaldt, R.A., Stone, E.C., and Vogt, R.E. 1975, Astrophys. J. Lett. **201**, 95.

Landau, L.D. 1946, J. Phys. (USSR) **10**, 25.

Lembege, B., and Dawson, J.M. 1989, Phys. Fluids B **1**, 1001.

Liewer, P.C., Lin, A. T., Dawson, J.M., and Caponi, M.Z. 1981, Phys. Fluids **24**, 1364.

Mason, G.M. 1987, Rev. Geophys. **25**, 1001.

Mason, G.M., Reames, D.V., Klecker, B., Hovestadt, D., and von Rosenvinge, T.T. 1986, Astrophys. J. **303**, 849.

Meyer, J.P. 1985a, Astrophys. J. Suppl. **57**, 151.

Meyer, J.P. 1985b, Astrophys. J. Suppl. **57**, 173.

Ohsawa, Y., and Dawson, J.M. 1984, Phys. Fluids **27**, 1491.

Ohsawa, Y. 1990, J. Phys. Soc. Jpn. **59**, 2782.

Ohsawa, Y., and Sakai, J-I. 1987, Astrophys. J. **313**, 440.

Reames, D.V. 1990, Astrophys. J. Suppl. **73**, 235.

Reames, D.V., Meyer, J.P., and von Rosenvinge, T.T. 1994, Astrophys. J. Suppl. **90**, 649.

Sarris, E.T., and Krimigis, S.M. 1985, Astrophys. J. **298**, 676.

Toida, M., and Ohsawa, Y. 1994, J. Phys. Soc. Jpn. **63**, 573.

Toida, M., and Ohsawa, Y. 1995, J. Phys. Soc. Jpn. **64**, 2038.

Toida, M., Ohsawa, Y., and Jyounouchi, T. 1995, Phys. Plasmas **2**, 3329.

Toida, M. , Zhang, T.X., and Ohsawa, Y. 1992, J. Phys. Soc. Jpn. **61**,3587.

Tokar, R.L., Gary, S.P., and Quest, K.B. 1987, Phys. Fluids **30**, 2569.

FIGURE CAPTIONS

FIG. 1. Dispersion curves for low- and high-frequency magnetosonic waves propagating perpendicular to a magnetic field in a plasma containing H and He. Ion density ratio is taken to be $n_{He}/n_H = 0.1$.

FIG. 2. Schematic diagram for wave profile and geometry. Here, $\widetilde{B}_z$ is the perturbed magnetic field, and Mv_h is the wave propagation speed.

FIG. 3. Magnetic field profiles of a nonlinear magnetosonic pulse at various times.

FIG. 4. Profiles of magnetic and electric fields and phase space plots $(x,\, v_y)$ of H, He, O, and Fe for a perpendicular magnetosonic pulse at $\omega_{pe}t = 1750$. Here, the magnetic field, electric fields, and velocities are normalized to B_o, $v_h B_o/c$, and v_h, respectively.

FIG. 5. Phase space plots $(v_x,\, v_y)$ of H, He, O, and Fe at $\omega_{pe}t = 1750$. Velocities are normalized to v_h.

FIG. 6. Profiles of magnetic and electric fields and phase space plots $(x,\, v_y)$ of H, He, O, and Fe for an oblique magnetosonic pulse at $\omega_{pe}t = 1700$. The angle between the wave normal and the ambient magnetic field is 50°.

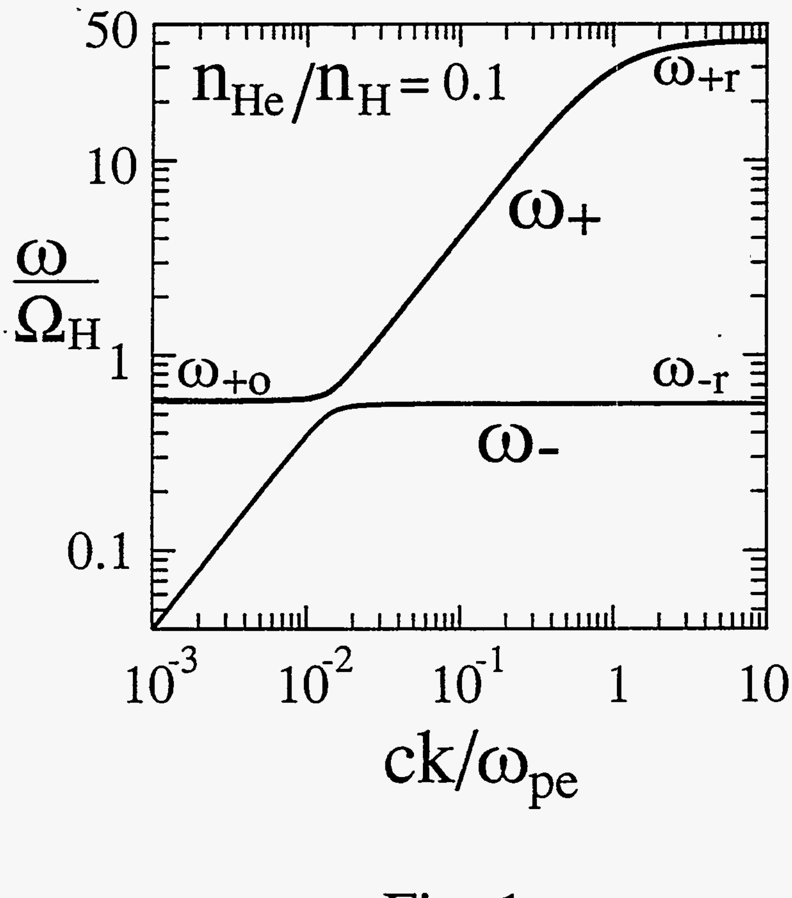

50
10
1
0.1
$n_{He}/n_H = 0.1$
ω_{+r}
ω_+
ω_{+o}
ω_{-r}
ω_-
$\frac{\omega}{\Omega_H}$
10^{-3}
10^{-2}
10^{-1}
1
10
ck/ω_{pe}

Fig. 1

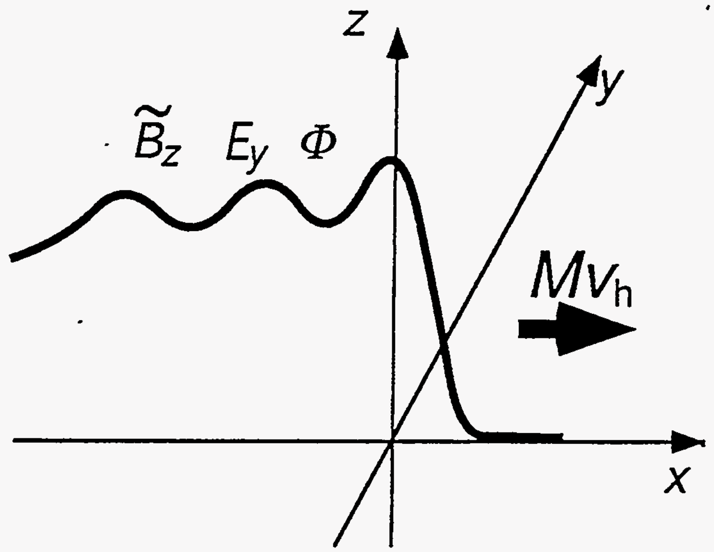

Fig. 2

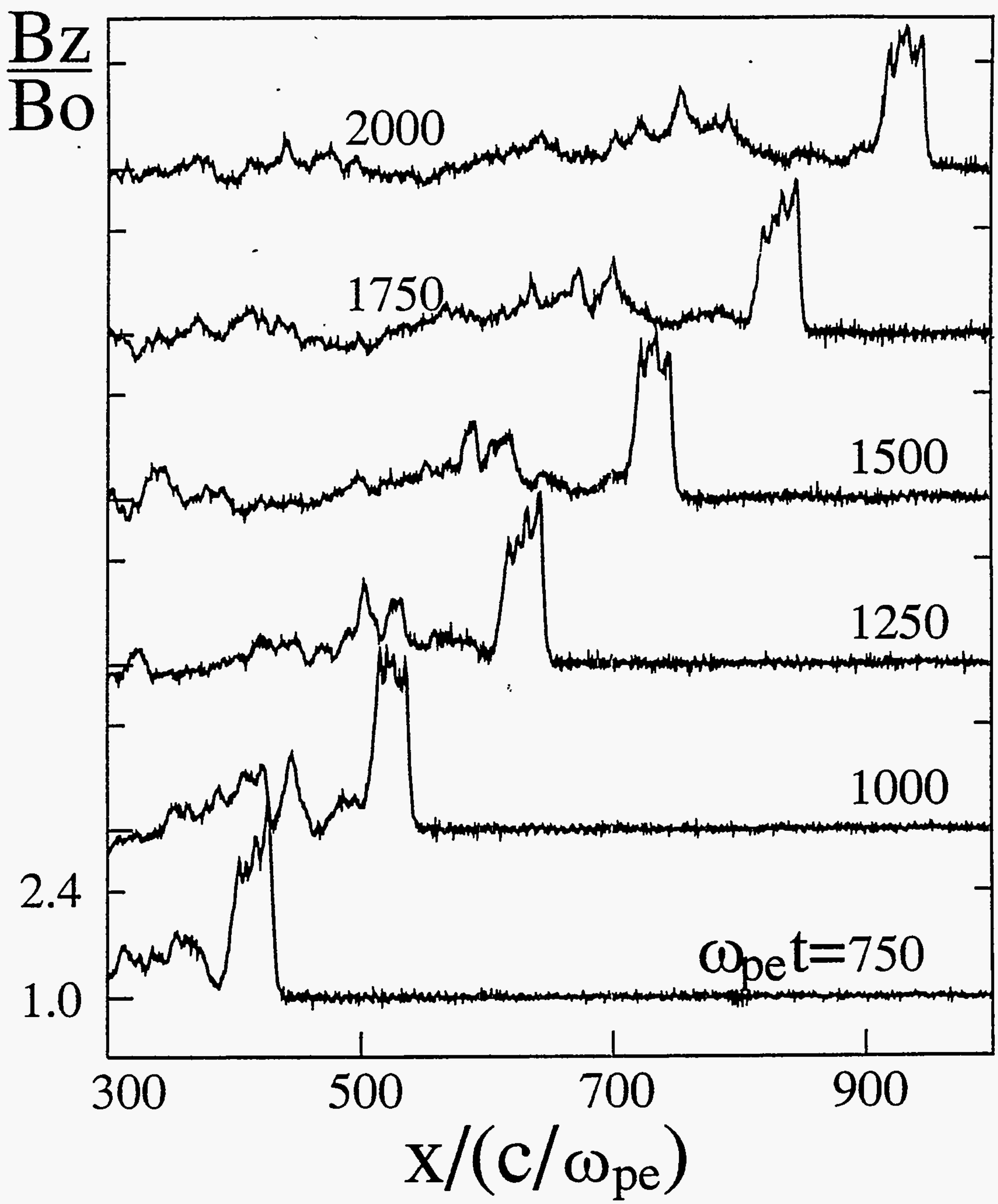

Bz
Bo
2000
1750
1500
1250
1000
2.4
$\omega_{pe}t=750$
1.0
300
500
700
900
$x/(c/\omega_{pe})$

Fig. 3

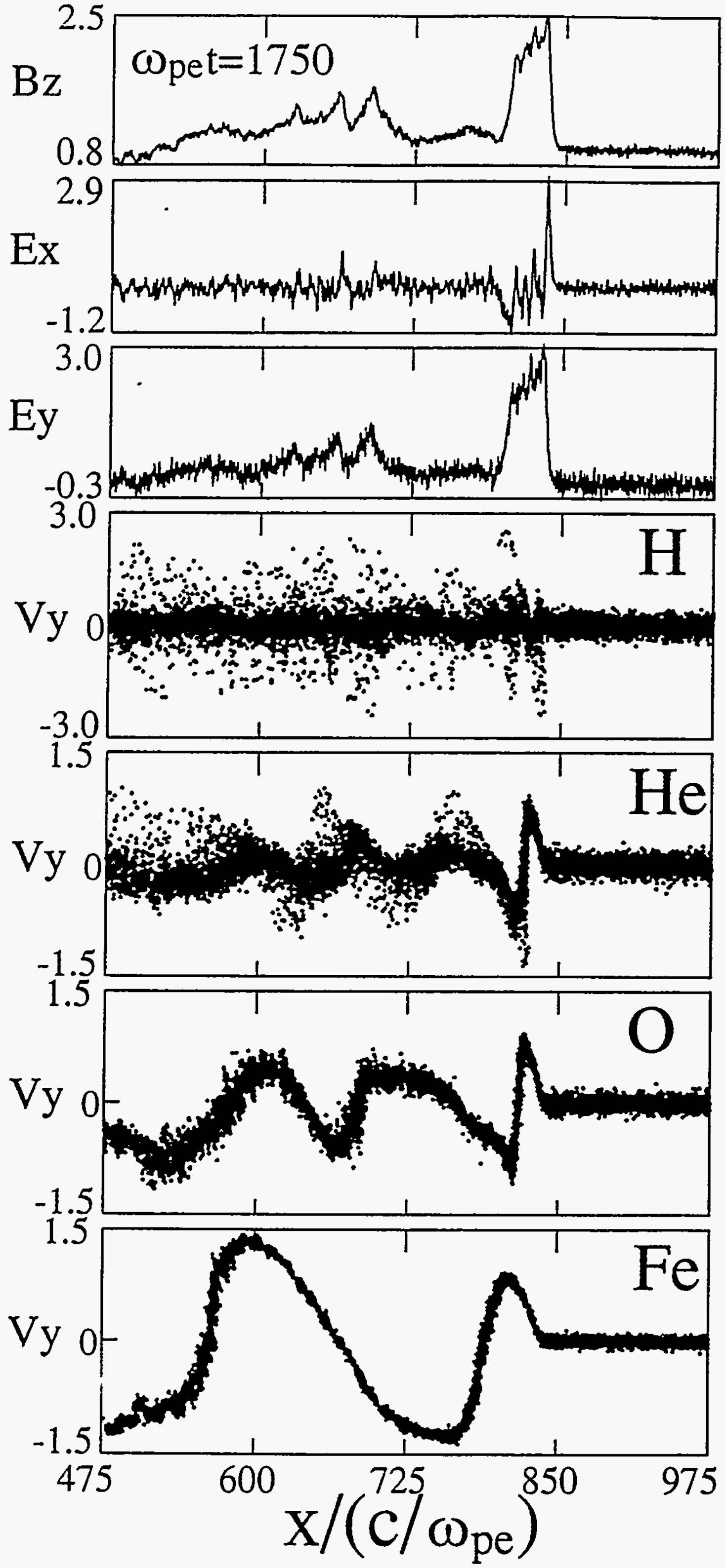

$\omega_{pe}t$=1750
Bz
2.5
0.8
Ex
2.9
-1.2
Ey
3.0
-0.3
H
Vy
3.0
0
-3.0
He
Vy
1.5
0
-1.5
O
Vy
1.5
0
-1.5
Fe
Vy
1.5
0
-1.5
475
600
725
850
975
$x/(c/\omega_{pe})$

Fig. 4

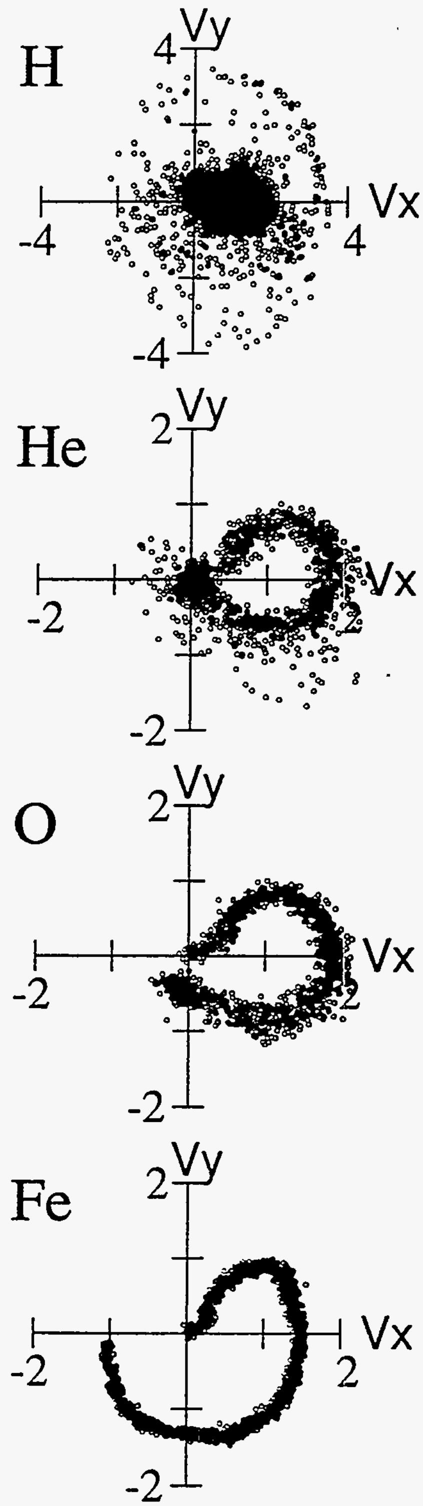

Fig. 5

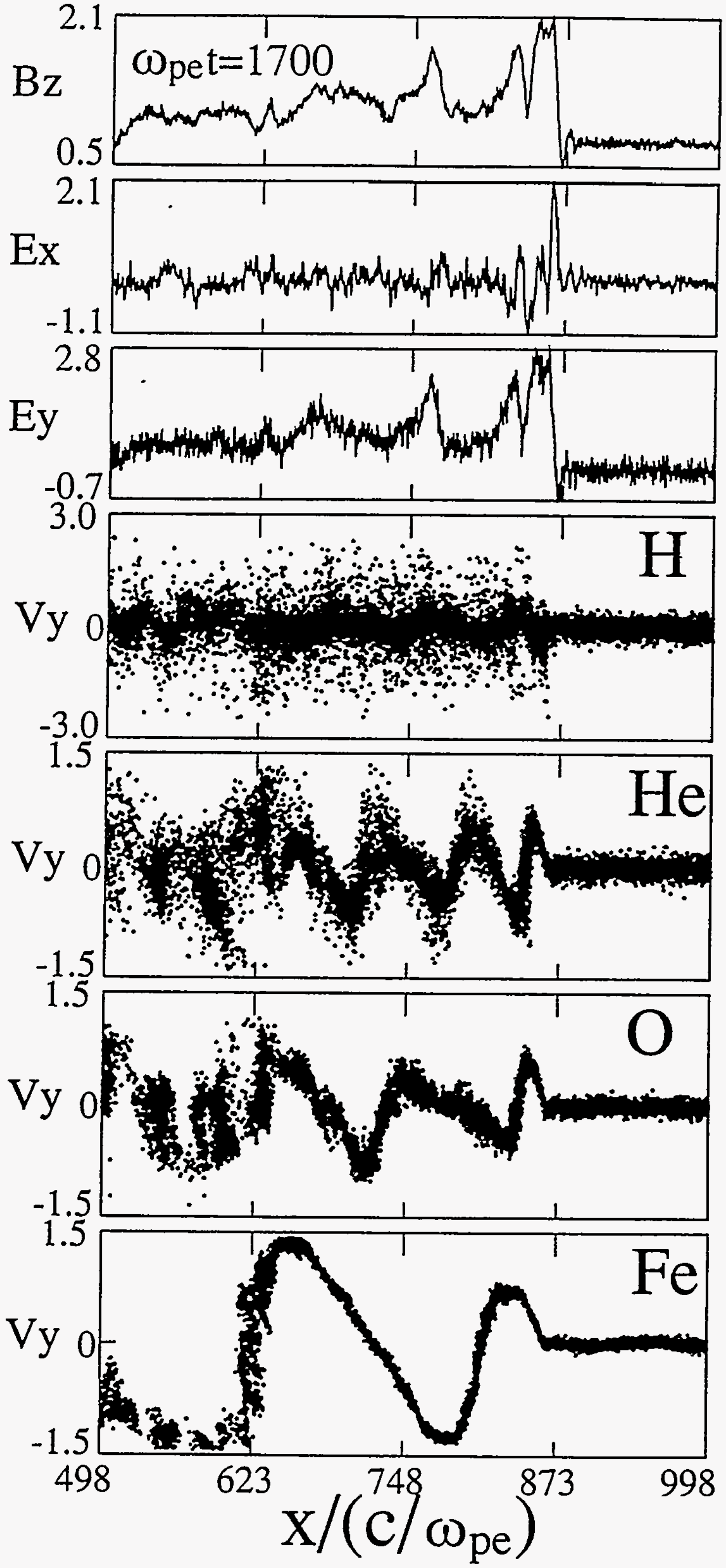

ωpet=1700
Bz
2.1
0.5
Ex
2.1
-1.1
Ey
2.8
-0.7
H
Vy
3.0
0
-3.0
He
Vy
1.5
0
-1.5
O
Vy
1.5
0
-1.5
Fe
Vy
1.5
0
-1.5
498
623
748
873
998
x/(c/ωpe)

Fig. 6